A Study of Evoked Potentials From Ear-EEG

Preben Kidmose*, *Senior Member, IEEE*, David Looney, *Member, IEEE*, Michael Ungstrup, *Member, IEEE*, Mike Lind Rank, *Member, IEEE*, and Danilo P. Mandic, *Fellow, IEEE*

***Abstract*—A method for brain monitoring based on measuring the electroencephalogram (EEG) from electrodes placed in-the-ear (ear-EEG) was recently proposed. The objective of this study is to further characterize the ear-EEG and perform a rigorous comparison against conventional on-scalp EEG. This is achieved for both auditory and visual evoked responses, over steady-state and transient paradigms, and across a population of subjects. The respective steady-state responses are evaluated in terms of signal-to-noise ratio and statistical significance, while the qualitative analysis of the transient responses is performed by considering grand averaged event-related potential (ERP) waveforms. The outcomes of this study demonstrate conclusively that the ear-EEG signals, in terms of the signal-to-noise ratio, are on par with conventional EEG recorded from electrodes placed over the temporal region.**

***Index Terms*—Auditory steady-state response (ASSR), ear-EEG, event-related potentials, evoked potentials (EP), steady-state visual evoked potentials (SSVEP).**

I. Introduction

ELECTROENCEPHALOGRAPHY (EEG) refers to the recording of electrical signals which represent aggregated electrical activity from a large number of temporally and spatially aligned neurons of the brain. The EEG signals typically originate from the cortex, but may also arise from the brainstem or from the cranial nerves. Within the clinical domain, EEG is a well-established and valuable tool for the diagnosis of e.g., neurological disorders, tumors, strokes, and brain death [1]. EEG is also extensively used within neurophysiology, cognitive neuroscience, cognitive psychology, and brain–computer interfacing (BCI) [2].

The characteristics of EEG signals depends on the location of the electrodes, the state of the brain, and the stimulation of the brain e.g. through the peripheral nervous system or the optic nerve/retina. An auditory stimulus, for instance, will induce modulated patterns into the EEG, and the changes in the EEG from the otherwise spontaneous EEG are termed auditory evoked potentials (EPs) [3].

Despite the clinical value of EEG, several issues limit its use beyond the clinical environment. To this end, a considerable effort went into the development of ambulatory and wearable EEG systems [4]. These allow for recording outside the clinical environment, but are largely inadequate for everyday use. This is both because of their limited ability to integrate into daily activities, requirement for a skilled assistant, and the fact that the ambulatory systems, like the conventional systems, still have clearly visible electrodes and leads from the electrodes to the recording device. Despite some advances in addressing these issues, on-scalp systems inevitably require a means for stable attachment (cap, headset, and/or adhesive), making the recording process uncomfortable, obtrusive, and stigmatizing.

Recently, we introduced a novel EEG recording approach called ear-EEG [5]–[7], whereby the signal is recorded from electrodes embedded on a personalized earpiece placed in the ear canal. Independently, a similar method was proposed in [8], where a more generic type of earpiece was disclosed. Whereas the ear-EEG method based on the individualized earpiece has been prototyped and validated, we are not aware of any results published from the method disclosed in [8].

Compared with existing on-scalp systems, the ear-EEG platform has several attractive properties [7]: discreet—not clearly visible or stigmatizing, unobtrusive—comfortable to wear and impeding the user as little as possible, and user-friendly—can be operated and attached by the user. In this way, ear-EEG exhibits a high degree of comfort and excellent long term wearability at the expense of a reduced number of electrodes and thus a compromise in recording quality. However, there are a number of applications, clinical and nonclinical, for which a small number of electrodes are sufficient, and for which a fully wearable recording platform is prerequisite.

So far ear-EEG has only been explored in proof-of-concept studies for a limited number of subjects [6]. Our aim is to further characterize the ear-EEG and compare it to conventional on-scalp EEG across a population of subjects. This is achieved through studies for both auditory and visual EPs, and for both steady state and transient responses.

II. Ear-EEG Recording Method and Setup

The basis of EEG is that a large number of spatially aligned neurons have coherent electrical activity. The dendrite current of the neurons causes a corresponding extracellular current that gives rise to electrical potentials in the tissue. These potentials are observable on the scalp surface and also on the surface of the ear canal. The feasibility of the ear-EEG concept is illustrated through a model of the propagation of the electrical potential from a spatially aligned and temporally synchronized group of neurons (approximated by a dipole) shown in Fig. 1.

The ear-EEG concept is illustrated in Fig. 2; electrodes made of silver (Ag) are embedded on a personalized earpiece placed

Manuscript received December 21, 2012; revised February 11, 2013 and May 22, 2013; accepted May 22, 2013. Date of publication May 29, 2013; date of current version September 14, 2013. *Asterisk indicates corresponding author.*

*P. Kidmose is with the Department of Engineering, Aarhus University, Aarhus DK-8000, Denmark (e-mail: pki@iha.dk).

D. Looney and D. P. Mandic are the with the Department of Electrical and Electronic Engineering, Imperial College, London SW7 2BT, U.K. (e-mail: david.looney06@imperial.ac.uk; d.mandic@imperial.ac.uk).

M. Ungstrup and M. L. Rank are with Widex A/S, Lynge DK-3540, Denmark (e-mail: miu@widex.com; mlr@widex.com).

Digital Object Identifier 10.1109/TBME.2013.2264956

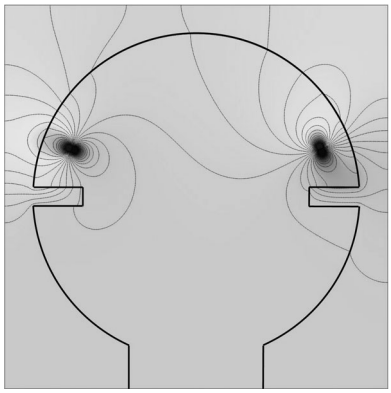

Fig. 1. Principle of the propagation of brain electrical potential to the scalp and ear canal from a population of neurons in the temporal region of the brain. The aggregated dendritic current from a large population of cortical neurons has been modeled as dipoles. The dipole on the left is radial (corresponding to neurons located on a gyrus), whereas the dipole on the right is tangential (corresponding to a dipole in a sulcus). Details: The simulation is 2-D. The head was modeled as a circle with radius 85 mm; the ear canals have height of 10 mm, and depth of 26 mm. The head was modeled as a homogeneous mass of tissue with conductivity 0.32 S/m corresponding to the conductivity of physiological saline. The dipole had an electric potential of -80 mV, corresponding to a typical cell membrane potential. The dimension of the dipole was 1×1 mm. The contour lines represent equipotentials with 50 μV between each line.

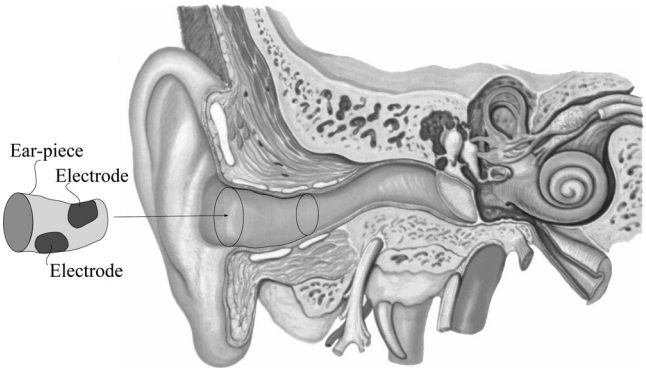

Fig. 2. Earpiece with embedded electrodes (relative to the ear canal).

in the outer ear. The earpieces in our study are produced using the same manufacturing processes as is standard for customized hearing aid earplugs: 1) taking a wax-impression of the outer ear; 2) obtaining a digitized 3-D model by scanning the impression in a 3-D laser-scanner; 3) modeling the earpiece in a CAD program; and 4) manufacturing of the earpiece using a 3-D printer (additive manufacturing technology). Electrodes are mounted on the outer surface of the earpiece and connected by leads to a connector embedded in the earpiece.

The earpieces are hollow, with a $\phi 3$ mm through-hole in the longitudinal direction for sound to propagate unimpeded to the eardrum. On each earpiece are placed four electrodes, and for all the recordings reported in this paper the electrode positions were ExA, ExB, ExE, and ExH for both x=L and x=R (see the labelling scheme in Appendix A). The electrode areas were approximately 20 mm^2; an example of an earpiece with electrodes is shown in Fig. 3(b) and (c).

For all the ear-EEG recordings, the electrode ExH was used as reference electrode, ExA was used as ground (common mode feedback), and the EEG signals were recorded from ExB and ExE relative to ExH. A distinguishing feature of our ear-EEG system is that the recordings are truly in-the-ear measurements; that is, all the electrodes, including the reference and ground electrodes, are placed within the ear, and are galvanically insulated from any of the electrode on the subject (e.g., scalp electrodes and electrodes in the opposite ear). Fig. 3(e) and (f) shows the experimental setup used, that allows for a simultaneous recording of ear-EEG and standard on-scalp EEG.

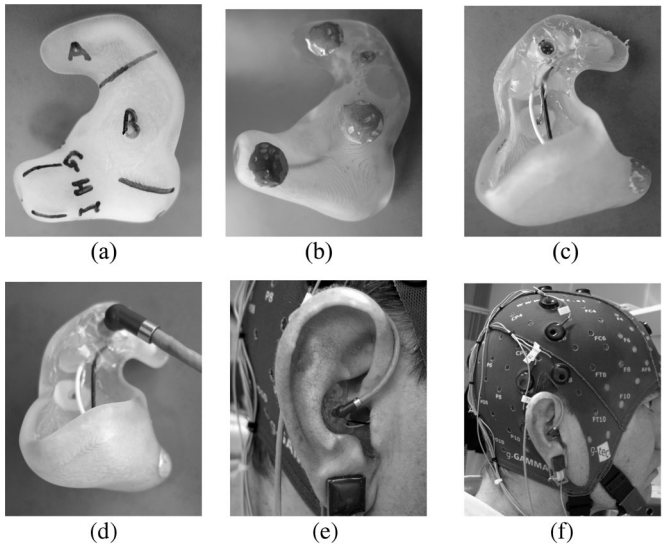

Fig. 3. Ear-EEG: Views of earplug for the right ear. (a) Right ear earplug marked with labels. (b) Earplug, electrodes ERA, ERB, and ERH are visible. (c) Opposite view to (b). Connector and electrode ERE are visible. (d) Earplug with the connector attached. (e) Right ear with the earplug in place. (f) Right side view of the measurement setup.

On-scalp EEG was recorded from eight electrodes (10–20 electrode system, electrode positions: T7, Tp7, Tp9, T8, Tp8, Tp10, Oz, and Pz) relative to the right ear lobe (reference) and the Cz electrode as ground (common mode feedback). The recording amplifier was the g.USBamp by g.tec, which allows simultaneous and independent (different ground and reference configurations) recordings of groups of EEG channels.

Before the recordings, the concha and the ear canals were cleaned with ethanol, and the skin was prepared with abrasive gel. Conductive gel was applied to the electrodes, the earpieces were put in place, and electrode impedances were tested to ensure that their values were below 5 kΩ.

III. Evoked Potentials: Methods and Stimuli

The amplitudes of EP are in general much lower than the amplitude of the spontaneous EEG, making it necessary to average over multiple trials in order to reveal the ERPs. However, since ERP waveforms typically last for several hundreds of milliseconds, the data segments used for the averaging often contain ERPs from previous stimuli. As a consequence, the averaged waveform will deviate from the true underlying ERP waveform, and this distortion may be significant even for rather long interstimulus intervals. A way to reduce this distortion is to apply a random interstimulus interval (jittered timing) which effectively

filters out the high frequency components from the underlying true ERP waveform. As the range of the random interstimulus interval is increased, the lower frequency aliasing components from the averaged waveform are reduced, see e.g., [9] for more detail.

Instead of trying to reduce the distortion caused by averaging, we can actively utilize this phenomenon by applying stimuli at a high and constant rate. The response will consequently change from an intricate, broadband transient response and into a steady-state response. The steady-state response is a periodic waveform comprised of complex exponentials at the stimulus repetition frequency and its multiples, and it can therefore be described as an amplitude and phase component at the stimulus repetition frequency and its multiples (i.e., a Fourier series). Since the steady-state response is frequency specific, it is easy to assess the significance of the response, but this comes at the cost of imprecise temporal information because of the inherent phase uncertainty.

For the analysis of the steady-state responses, the EEG signals were bandpass filtered to the frequency interval 1–100 Hz, and a notch filter at the first, second, and third harmonics of the 50 Hz power line frequency was applied. The evoked response was estimated by averaging 256 nonoverlapping segments of 1 s in duration. Along with the evoked response, the noise signal was estimated by altering the sign of the data in every other segment of the averaging, thereby eliminating the deterministic (evoked) part of the signal. For every doubling of the number of segments in the averaging the signal-to-noise ratio (SNR) increases by 3 dB; thus, the averaging performed here results in an increase in the SNR of 24 dB relative to no averaging. For the analysis of the transient responses, the EEG signals were bandpass filtered to the frequency interval 1–20 Hz, and a notch filter at the first, second, and third harmonics of the 50 Hz power line frequency was applied. The evoked response was estimated by splitting up the signal in 256 nonoverlapping segments of 1 s in duration, removing the 26 segments with the highest standard deviation, and averaging the remaining 230 segments.

A. Auditory Steady-State Response

Auditory steady-state responses (ASSR) were first reported in [10], and have since been extensively studied, primarily as an objective assessment of the hearing threshold level [11]. The ASSRs can be evoked by different types of stimuli, typically amplitude modulated narrow- or broad-band signals [3]. The sound stimulus used to induce the ASSR in our study was amplitude-modulated white Gaussian noise, with both 40 and 80 Hz amplitude modulation (SPL 69.4 dB RMS rel. 20 μPa). EEG was recorded simultaneously from eight on-scalp and four ear-EEG electrodes, and for eight different subjects.

B. Steady-State Visual Evoked Potential

The steady-state visual evoked potentials (SSVEP) have been considered in many areas, from the investigation of the human visual system in early behavioral studies [12], through objective threshold studies based on EEG recordings [13], to pathological studies in, e.g., Alzheimer and Parkinson patients [14]. The human visual system can perceive modulation in light intensity at frequencies up to approximately 75 Hz (strongly dependent on light intensity), and it is most sensitive in the region around 10 Hz [12]. The SSVEP is typically induced by either amplitude modulated or flashing light, and the EEG signals are typically recorded from occipital and parietal region electrodes. The SSVEP in our study was induced by flashing light with frequencies of 10, 15, and 20 Hz and at a 50% duty cycle. The EEG was recorded using the same setup as described in the previous sections and over six subjects.

C. Transient Auditory Evoked Potential

The auditory evoked $P_1 - N_1 - P_2$ complex is an ERP evoked by a sound stimulus and is attributed to the processing within in or near the auditory cortex [3]. The presence of auditory ERPs indicates that the stimulus has been detected at the level of the auditory cortex, but does not in general provide information regarding cognitive discrimination.

The sound cue (event) used for the $P_1 - N_1 - P_2$ complex recordings was a 1 kHz sinusoid of duration 200 ms, with an attack and release time of 10 ms. The interstimulus interval was randomly chosen in between 1.7 and 2.3 s. The presentation of the sound stimulus and the EEG recording setup was the same as in the previous sections.

D. Transient Visual Evoked Potential

The visual evoked potential (VEP) from pattern onset is attributed to processing in the primary visual cortex, and these onset responses can be observed from many locations across the scalp [15]. To explore VEP from ear-EEG recordings, we used the same EEG recording setup as in the previous studies and the same light stimulation source as for the SSVEP study. Each stimulus had duration of 5 ms with a random interstimulus interval uniformly distributed between 300 and 500 ms; the VEP waveform was obtained by averaging 500 ms nonoverlapping segments.

E. Stimuli

The auditory stimuli were presented binaurally using headphones, the setup was gain calibrated at 1 kHz, and all stimuli were presented with maximum amplitude corresponding to a sound pressure level (SPL) of 80 dB relative to 20 μPa. The headphones were Beyerdynamic DT 770 PRO (250 Ω) driven by a ESI Dua Fire soundcard; the audio setup was calibrated using a Bruel&Kjær Head and Torso Simulator, Type 4128C, equipped with IEC 711 ear couplers. All sound stimuli were generated digitally with 24 bit resolution and at 44.1 kHz sampling rate. The visual stimuli were presented by an array of 3 $\times$ 3 white 5 mm LEDs at a distance of approximately 25 cm from the subject.

IV. Results

In the following, we provide a comprehensive quantitative and qualitative characterization of the ear-EEG and a comparative analysis against conventional on-scalp EEG by considering both

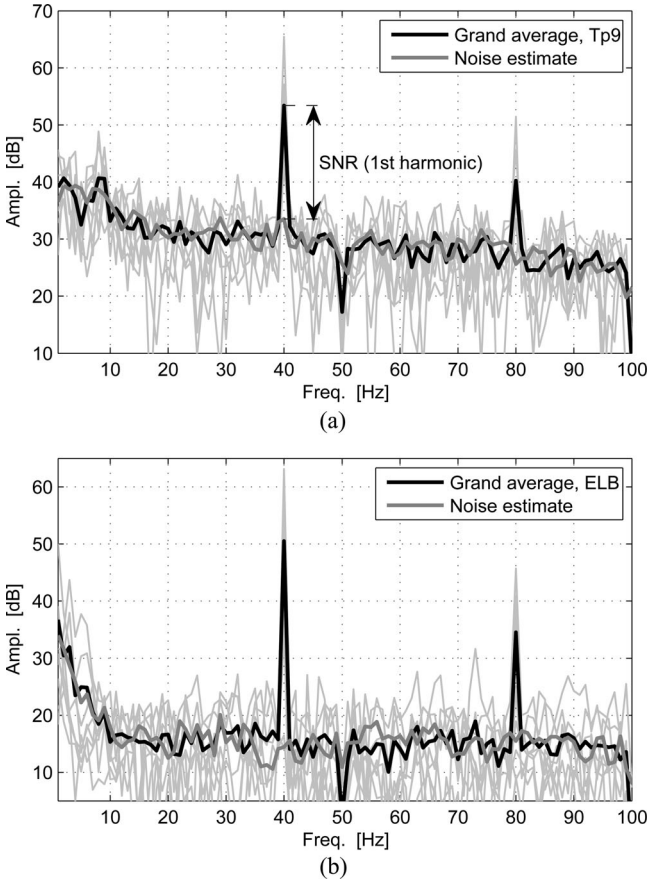

Fig. 4. Grand average power spectrum of the auditory steady-state response evoked by white Gaussian noise amplitude-modulated with a 40 Hz sinusoid. The thin lines denote the power spectra of the eight subjects. (a) ASSR for the left temporal lobe, electrode TP9. (b) ASSR for the left ear, electrode ELB.

transient and steady-state characteristics of auditory and visual EPs.

A. Auditory Steady-State Response

For steady-state responses it is natural to consider the power spectrum, i.e., the squared absolute value of the Fourier transform of the time-domain waveform. Fig. 4 shows the power spectra for the ASSR with 40 Hz modulation (amplitudes relative to 1 μV, frequency resolution 1 Hz); the top panel shows the results for the scalp electrode (Tp9), and the bottom panel for the ear electrode (ELB). The bold lines denote the grand average of the ASSR and the noise estimate, while the thin lines are the ASSRs of the 8 subjects. The first and the second harmonic component (of the modulation frequency) are prominen in both spectra; for the Tp9 electrode the SNR at the first harmonic component was approximately 20 dB, whereas for the ELB electrode the SNR was approximately 35 dB. It is observed that for the ear-EEG the overall signal level is 15–20 dB lower compared to the on-scalp recording. However, as the SNR increased relative to the scalp electrodes we conclude that the lower signal amplitudes of the ear electrodes did not compromised the signal quality. The lower signal amplitudes of ear-EEG are largely due to significantly shorter electrode distances compared to conventional on-scalp recordings, which is supported by the simulation in Fig. 1, but may also be affected by a thicker bone structure between the brain and the surface of the ear canal compared to the bone structure between the brain and the surface of the scalp where conventional electrodes are placed, as shown in Fig. 2.

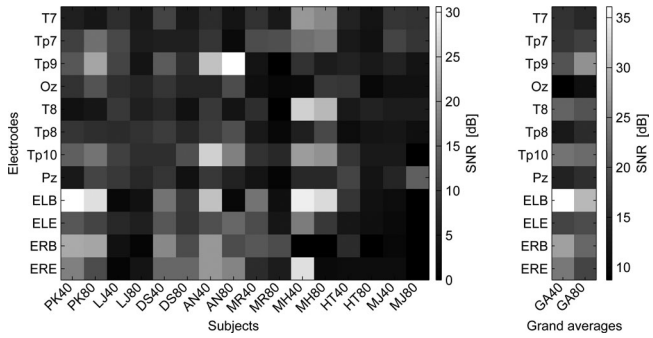

Fig. 5. Left panel: Signal to noise ratio of the first harmonic component of the ASSR for eight different subjects and for two different stimulus frequencies (40 and 80 Hz). Right panel: Grand average SNR over the eight subjects.

The left panel of Fig. 5 shows the SNR for the first harmonic component obtained for 8 subjects, 12 electrode positions, and 2 modulation frequencies (40 and 80 Hz); the right panel shows the grand average SNR for the first harmonic component (averaging over subjects). It is observed that there are significant variations in the SNR across subjects, but for a given subject the on-scalp and ear electrodes have similar performances; i.e., high SNRs in the on-scalp electrodes are typically matched by high SNRs in the in-the-ear electrodes, and vice versa. Table I shows the mean values of the SNR for the on-scalp EEG and the ear-EEG and also the grand average SNR over both subjects and electrodes. It is observed that the mean SNRs were largest for the ear recordings in 9 out of 16 subjects, and the grand average SNRs were also largest for the ear electrodes for both modulation frequencies.

For rigour, we also calculated the statistical significance of the first-order component as a one-tailed *t*-test, where the null hypothesis was that the mean of the noise is equal to the mean value of the signal. The mean values were obtained by subdividing the 256 segments considered into 16×16 segments, averaging over 16 segments, and calculating the mean and the standard deviation for both the signal and the noise from 16 of these averages. The (p-1)-values of this statistical significance analysis are shown in Fig. 6. For three out of the eight subjects (LJ, HT, and MJ) the statistical significance was lower for the ear electrodes, while for the remaining five subjects the significance for the ear electrodes was comparable to that of the scalp electrodes.

B. Steady-State Visual Evoked Potential

The SSVEP can be observed from many locations along the scalp and, as shown next, this also includes the temporal region electrode (Tp9) and the in-the-ear electrodes (ELB). Fig. 7 shows the power spectra for the 10 Hz SSVEP experiment for three different electrode positions: parietal lobe (Pz) [see Fig. 7(a)], temporal lobe (Tp9) [see Fig. 7(b)], and in-the-ear

TABLE I
AVERAGE SNR ([dB]) FOR THE SCALP- AND EAR-ELECTRODES OF THE FIRST HARMONIC COMPONENT OF THE ASSR STUDY

Recording	PK40	PK80	LJ40	LJ80	DS40	DS80	AN40	AN80	MR40	MR80	MH40	MH80	HT40	HT80	MJ40	MJ80	GA40	GA80
On-scalp	10.0	15.6	**9.4**	**6.1**	9.6	7.3	19.6	**22.0**	7.0	5.6	19.3	17.6	**7.2**	**4.3**	**6.7**	**8.2**	17.9	19.3
Ear	**25.1**	**22.7**	3.5	3.8	**16.1**	**11.8**	**21.3**	14.7	**13.5**	**6.9**	**25.7**	**21.2**	6.6	2.5	1.9	0.0	**29.0**	**23.7**
Difference	-15.1	-7.3	5.7	2.8	-6.7	-4.7	1.4	7.2	-6.0	-1.6	-6.2	-3.3	0.8	1.9	5.0	8.1	-11.1	-4.4

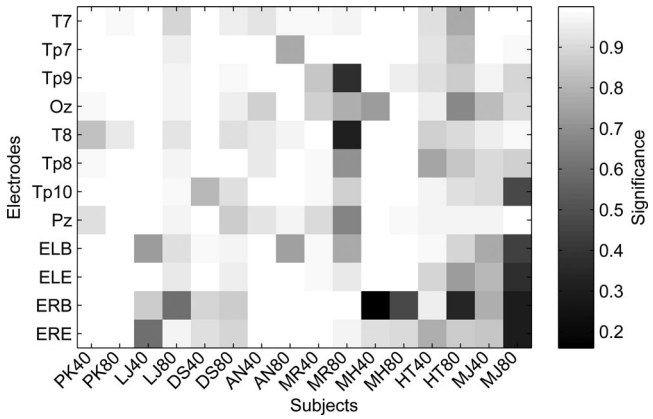

Fig. 6. Statistical significance of the first harmonic component of the ASSR study over eight different subjects and two different stimuli (95% significance level).

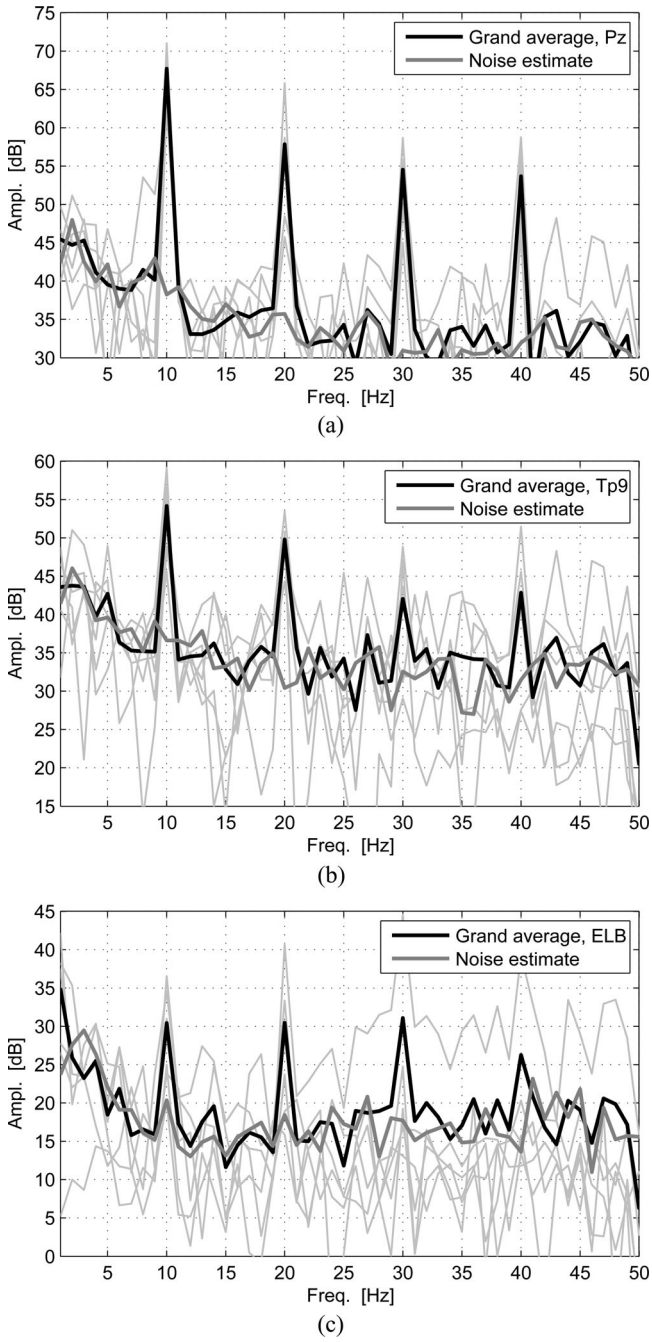

Fig. 7. Grand average power spectra for the 10 Hz SSVEP experiment. (a) SSVEP for the parietal lobe, electrode Pz. (b) SSVEP for the left temporal lobe, electrode Tp9. (c) SSVEP for the left ear, electrode ELB.

(ELB) [see Fig. 7(c)]. The bold lines show the grand average of the SSVEP and the noise estimates, while the thin lines are the SSVEPs for the six subjects. In the grand average SSVEP power spectra the harmonics of the modulation frequency are clearly visible in all electrode positions. The Pz recordings had a grand average SNR at the first harmonic component of approximately 30 dB, and for the Tp9 and ELB recordings this decreased to approximately 17 and 10 dB respectively. Thus, for the SSVEP experiments the signal quality was lower for the ear electrodes compared to the scalp electrodes. As was the case for the ASSR study, the ELB recording had a noise floor that was approximately 20 dB lower than that of the scalp recordings.

Similarly to the ASSR study, the estimated SNR of the first harmonic component of the SSVEP for all electrodes and all subjects, together with grand averages, are summarized in Fig. 8. Consistent with the previous analysis, the ear-EEG recordings in general had a lower SNR compared to the scalp electrodes, however a statistical significance analysis, similar to that for the ASSR study in Fig. 6, showed that the SSVEP were significant for all the subjects.

C. Transient Auditory Evoked Potential

Examples of AEP waveforms recorded from a Tp9 and an ELB are shown in Fig. 9. The bold lines show the grand averaged waveform, and the gray lines the EPs for subjects: PK, LJ and MJ. Consistent with the findings for the ASSR and SSVEP studies, the amplitudes of the ear-recording were approximately 10 times lower (corresponding to $-$ 20 dB) compared to the on-scalp recording. It is observed that the ear-EEG waveform is very similar to the on-scalp EEG waveform, thus demonstrating the feasibility of obtaining transient responses from ear-EEG recordings. We have also found that the SNR (i.e. the ratio between the amplitude of the waveform and the standard deviation) was smaller for the ear-EEG recording compared to the on-scalp

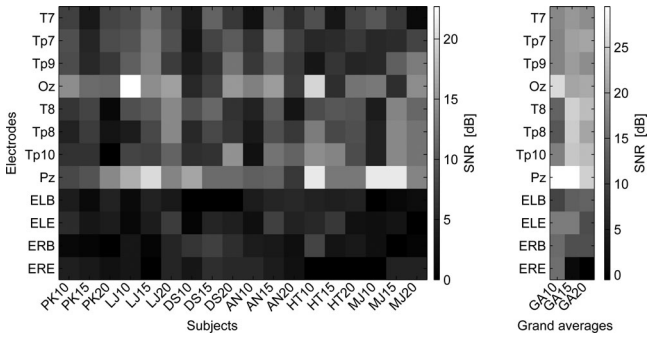

Fig. 8. Left panel: SNR [dB] of the first harmonic component of the SSVEP study over six different subjects and three different stimulus frequencies. Right panel: Grand average SNR over the six subjects for the three different stimulus frequencies.

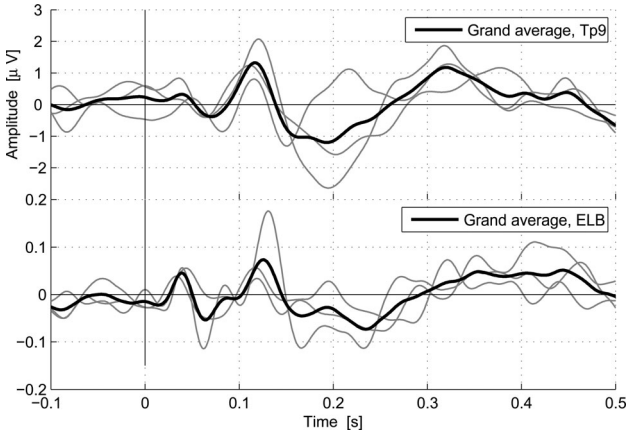

Fig. 9. Auditory evoked potential induced by a 1 kHz tone cue of duration 200 ms with an attack and release time of 10 ms. Stimuli were presented at the same time in the left and right ear, and the inter-stimulus-interval was randomly selected within the range 1.7 to 2.3 s. The figure shows the EPs for electrode positions Tp9 and ELB; bold lines show the grand average, and gray lines the EPs for subject PK, LJ, and MJ.

EEG recording; this is primarily due to amplifier noise, rather than an inherent characteristic of the ear-EEG (amplifier noise was measured using a balanced resistor triangle with 4320 Ω resistors, showing 0.47 μV/$\sqrt{\text{Hz}}$).

D. Transient Visual Evoked Potential

Fig. 10 shows examples of VEP waveforms recorded from the occipital region (Oz), Tp9, and ELB. The bold lines show the grand averaged waveforms, and the gray lines the EPs for subjects: PK, LJ and MJ. Consistent with the above findings, the amplitude of the ear-EEG recording was approximately 20 dB lower compared to on-scalp recordings. However, it is important to notice that a waveform similar to the on-scalp EEG can be observed from the ear-EEG, thus demonstrating the feasibility ear-EEG based VEP. As for the transient AEP, the SNR was lower for ear-EEG recordings compared to on-scalp EEG.

V. Conclusion

This study has addressed the feasibility of the novel ear-EEG recording method through a comprehensive validation against

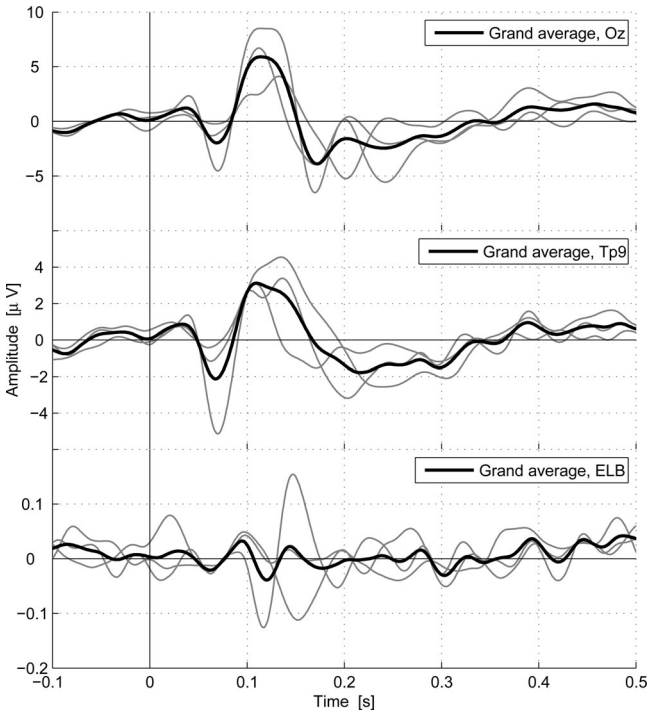

Fig. 10. Visual evoked potentials induced by a high intensity white LED array, with stimulus duration of 5 ms and an interstimulus interval randomly selected between 300 and 500 ms. The figure shows the EP for electrode positions Oz, Tp9 and ELB. The bold lines show the grand average, while the gray lines are the EPs for subjects: PK, LJ and MJ.

conventional on-scalp EEG. This has been achieved over four different event-related potentials (ERP) and across a group of 6–8 subjects. The ERPs considered were: ASSR, SSVEP, an auditory evoked $P_1 - N_1 - P_2$ complex, and a visual evoked onset response. It has been observed that the signal level in the ear-EEG in general is approximately 20 dB lower in amplitude compared to the conventional EEG. However, for steady-state responses, despite the lower signal levels, the signal to noise ratio, and thus the signal quality, is in general maintained. For transient responses, the ear-EEG waveforms resembled the waveforms observed from the temporal lobe electrodes; the transient responses obtained from ear-EEG had lower SNR compared to conventional on-scalp EEG which is attributed to amplifier noise rather than an inherent characteristic of ear-EEG. A comprehensive statistical significance validation of ear-EEG, combined with its unique advantages (noninvasive, unobtrusive, user friendly, and discreet), has established the basis for the use of ear-EEG in applications in which limited spatial resolution is sufficient and continuous monitoring is a prerequisite.

Appendix A

Labelling Scheme for Naming Ear-EEG Electrodes

The in-the-ear electrodes are denoted by Exy where x $\in$ $\{\text{L, R}\}$ denotes electrodes in the left and right ear, respectively, and y denotes the electrode position in the ear. In each ear, we define 12 electrode positions, denoted by letters from A to L, that is y $\in \{\text{A, B}, \ldots, \text{L}\}$. The letters A, B, and C denote electrode

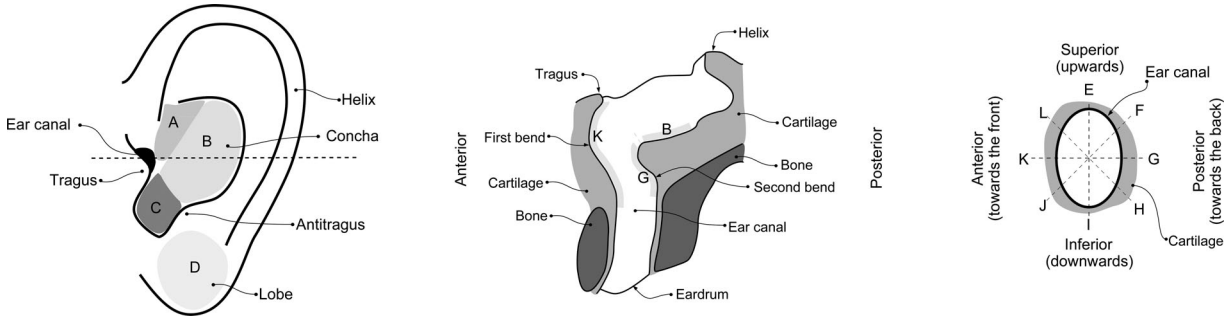

Fig. 11. Ear electrode labelling scheme for the left ear. (Left) Sketch of the exterior part of the ear, showing the four regions corresponding to the electrode labels A through D. (Center) Cross-sectional sketch of the outer ear in the axial plane, the drawing cut is indicated by a dashed line in the left figure, electrode positions B, G, and K are indicated. (Right) Cross-sectional view of the ear canal (sagital plane) showing the electrode labels in the ear canal. The electrodes are labelled based on the direction relative to the vertical axis, and not based on the depth in the ear canal.

positions in the concha part of the ear; the letter D denotes the ear lobe electrode, and the letters E through L denote electrode positions in the ear canal. The labelling scheme is illustrated in Fig. 11 for the left ear, the same labelling scheme applies to the right ear. For instance, electrode ERB is an electrode placed in the concha region of the right ear. Fig. 3(a) shows a photo of a blank earpiece with the electrode positions indicated. The electrodes in the ear canal are located before the bony part of the ear canal (see also Fig. 2), and the electrode position is defined by the direction (angle) of the electrode relative to the vertical axis. The vertical axis is defined as perpendicular to the plane defined by the Oz, FPz, and T7/T8 electrode positions (as defined by the 10–20 electrode position system).

REFERENCES

[1] M. J. Aminoff, *Electrodiagnosis in Clinical Neurology*, 5th ed. U.K.: Elsevier, 2005.
[2] J. Wolpaw, N. Birbaumer, W. Heetderks, D. McFarland, P. Peckham, G. Schalk, E. Donchin, L. Quatrano, C. Robinson, and T. Vaughan, "Brain-computer interface technology: A review of the first international meeting," *IEEE Trans. Rehabil. Eng.*, vol. 8, no. 2, pp. 164–173, Jun. 2000.
[3] R. F. Burkard, M. Don, and J. J. Eggermont, *Auditory Evoked Potential: Basic Principles and Clinical Application*. Baltimore, MD, USA: Williams & Wilkins, 2007.
[4] A. Casson, D. Yates, S. Smith, J. Duncan, and E. Rodriguez-Villegas, "Wearable electroencephalography," *IEEE Eng. Med. Biol. Mag.*, vol. 29, no. 3, pp. 44–56, May/Jun. 2010.
[5] D. Looney, C. Park, P. Kidmose, M. L. Rank, M. Ungstrup, K. Rosenkranz, and D. P. Mandic, "An in-the-ear platform for recording electroencephalogram," in *Proc. Int. Conf. IEEE Eng. Med. Biol. Soc.*, 2011, pp. 6682–6885.
[6] P. Kidmose, D. Looney, and D. P. Mandic, "Auditory evoked responses from Ear-EEG recordings," in *Proc. Int. Conf. IEEE Eng. Med. Biol. Soc.*, 2012, pp. 586–589.
[7] D. Looney, P. Kidmose, C. Park, M. Ungstrup, M. Rank, K. Rosenkranz, and D. Mandic, "The in-the-ear recording concept," *IEEE Pulse*, vol. 3, no. 6, pp. 32–42, Nov./Dec. 2012.
[8] R. J. Fischer, J. Ferraro, P. Lal, and H. Lusted, "Apparatus and method for the measurement and monitoring of bioelectric signal patterns," Patent Application. Pub. No.: US 2007/0112277, Filed Oct. 16, 2006.
[9] M. G. Woldorff, "Distortion of ERP averages due to overlap from temporally adjacent ERPs: Analysis and correction," *Psychophysiology*, vol. 30, pp. 98–119, 1993.
[10] R. Galambos, S. Makeig, and P. J. Talmachoff, "A 40-Hz auditory potential recorded from the human scalp," *Proc. Natl. Acad. Sci. USA*, vol. 78, no. 4, pp. 2643–2647, 1981.
[11] B. Cone-Wesson, R. C. Dowell, D. Tomlin, G. Rance, and W. J. Ming, "The auditory steady-state response: Comparisons with the auditory brainstem response," *J. Amer. Acad. Audiol.*, vol. 13, no. 4, pp. 173–187, 2002.
[12] H. D. L. Dzn, "Research into the dynamic nature of the human fovea-cortex systems with intermittent and modulated light. I. Attenuation characteristics with white and colored light," *J. Opt. Soc. Amer.*, vol. 48, no. 11, pp. 777–784, 1958.
[13] L. H. Van der Tweel and H. F. E. Verduyn Lunel, "Human visual responses to sinusoidally modulated light," *Electroencephalogr. Clin. Neurophysiol.*, vol. 18, pp. 587–598, 1965.
[14] F. Vialatte, M. Maurice, J. Dauwels, and A. Cichocki, "Steady-state visually evoked potentials: Focus on essential paradigms and future perspectives," *Progr. Neurobiol.*, vol. 90, no. 4, pp. 418–438, 2010.
[15] F. D. Russo, A. Martinez, M. I. Sereno, S. Pitzalis, and S. A. Hillyard, "Cortical sources of the early components of the visual evoked potential," *Human Brain Mapp.*, vol. 15, pp. 95–111, 2001.

Preben Kidmose (SM'12) received the M.Sc. degree in engineering in 1998, and the Ph.D. degree in signal processing in 2001 from the Technical University of Denmark, Lyngby, Denmark.

He is currently a Professor (Ingeniørdocent) in biomedical engineering with the Department of Engineering, Aarhus University, Aarhus, Denmark. His research interest include signal processing in medical devices, audio signal processing, machine learning, medical instrumentation, and biomedical system engineering/design.

David Looney (M'08) received the B.Eng. degree in electronic engineering from University College Dublin, Dublin, Ireland, and the Ph.D. degree in signal processing from Imperial College, London, U.K., in 2011.

He is currently a Research Associate in the Communications and Signal Processing Group, Department of Electrical and Electronic Engineering, Imperial College, London. His research interests are in the areas of data fusion, time-frequency analysis, matrix factorization, and wearable solutions for health-monitoring.

Michael Ungstrup (M'09) received the M.Sc. degree in electrical engineering from the Technical University of Denmark in 1998.

He is currently with Widex A/S, Denmark. His research interest include signal processing and machine learning for audio applications and communication.

Mike Lind Rank (M'95) received the M.Sc. degree in electrical engineering in 1994, and the Ph.D. in control theory in 1998 from the Technical University of Denmark, Lyngby, Denmark.

He is currently with Widex A/S, Lynge, Denmark. His research interests include signal processing and machine learning for audio applications and communication.

Danilo P. Mandic (F'13) received the M.Eng degree in electronic engineering and the M.Sc degree in signal processing from the University of Banjaluka, Yugoslavia, in 1987 and 1992, respectively, and the Ph.D degree in signal processing from Imperial College London, U.K., in 1999.

He is a Professor in signal processing at Imperial College, London, U.K. His research areas include nonlinear multidimensional adaptive modeling, system identification and prediction, one- and multi-dimensional adaptive denoising, blind source separation and extraction, brain signal processing, sensor fusion, and signal modality characterization. His publication includes two research monographs, two edited books, and more than 200 publications on signal and image processing.